

Simulation of Electrochemical Aptamer-Based Sensors: A Kinetic and Binding Model Perspective

A Haghghatbin

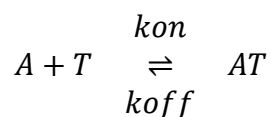
Electrochemical aptamer-based sensors represent a rapidly evolving class of biosensors that exploit the specific binding properties of nucleic acid aptamers to detect target molecules. The operation of these sensors is intrinsically linked to the conformational dynamics of the aptamer and its subsequent modulation of electron transfer kinetics. This article provides an overview of the simulation of such sensors, detailing the derivation of the governing kinetic equations, the relationship between these equations and the Hill–Langmuir isotherm, and the factors that contribute to the characteristic sigmoidal binding curves observed in experimental data. By integrating fundamental principles of chemical kinetics with established binding models, the simulation framework elucidates the operational mechanisms of these sensors and offers insight into their optimisation and performance evaluation.

Electrochemical aptamer-based sensors have emerged as a significant technological innovation in the field of biosensing. Unlike conventional antibody-based systems, aptamers are synthetic oligonucleotides that can be engineered to recognise a wide array of targets, including proteins, small molecules, and even cells. Their stability, ease of synthesis, and capacity for conformational modulation upon target binding render them particularly attractive for incorporation into electrochemical sensing platforms. The core principle of these sensors lies in the translation of a molecular recognition event into a measurable electrical signal, primarily through changes in electron transfer rates induced by aptamer conformational changes.

Understanding and simulating the behaviour of electrochemical aptamer-based sensors is crucial for advancing their design and application. Simulation not only allows for the prediction of sensor responses under various conditions but also aids in the optimisation of sensor parameters, such as binding kinetics and electron transfer efficiency. In this context, the derivation of the underlying kinetic equations and the incorporation of binding models such as the Hill–Langmuir isotherm is fundamental to a robust simulation framework.

Kinetic Modelling of Aptamer–Target Interactions

At the heart of the simulation of electrochemical aptamer-based sensors is the kinetic model that describes the binding interaction between the aptamer and its target. The reaction is typically represented as a simple reversible binding process:



Here, A denotes the aptamer, T represents the target molecule, and AT is the aptamer–target complex. The rate constants k_{on} and k_{off} govern the forward (binding) and reverse (dissociation) reactions, respectively.

The application of the law of mass action to this system stipulates that the rate of the forward reaction is proportional to the product of the concentrations of the free aptamer and the target:

$$\text{Rate}_{\text{forward}} = k_{\text{on}} \cdot [A] \cdot [T]$$

Similarly, the rate of dissociation is proportional to the concentration of the formed complex:

$$\text{Rate}_{\text{reverse}} = k_{\text{off}} \cdot [\text{AT}]$$

Thus, the net rate of formation of the complex $[\text{AT}]$ is given by the difference between these two rates:

$$\frac{d[\text{AT}]}{dt} = k_{\text{on}} \cdot [\text{A}] \cdot [\text{T}] - k_{\text{off}} \cdot [\text{AT}]$$

To account for the conservation of the total aptamer concentration, we introduce A_{Total} where

$$A_{\text{total}} = [\text{A}] + [\text{AT}]$$

Thus, the concentration of free aptamer is expressed as:

$$[\text{A}] = A_{\text{total}} - [\text{AT}]$$

Substituting this into the net rate equation yields:

$$\frac{d[\text{AT}]}{dt} = k_{\text{on}} \cdot (A_{\text{total}} - [\text{AT}]) \cdot [\text{T}] - k_{\text{off}} \cdot [\text{AT}]$$

This differential equation forms the cornerstone of the simulation model, capturing the time-dependent kinetics of the aptamer–target binding process. While the differential equation derived above provides a dynamic description of binding, its steady-state solution is intimately connected to the well-known Hill–Langmuir isotherm. At equilibrium, where $\frac{d[\text{AT}]}{dt} = 0$ the rate of association equals the rate of dissociation:

$$k_{\text{on}} \cdot (A_{\text{total}} - [\text{AT}]) \cdot [\text{T}] = k_{\text{off}} \cdot [\text{AT}]$$

Rearranging this equation allows one to solve for the equilibrium concentration $[\text{AT}]_{\text{eq}}$

$$[\text{AT}]_{\text{eq}} = \frac{k_{\text{on}} A_{\text{total}} [\text{T}]}{k_{\text{off}} + k_{\text{on}} [\text{T}]}$$

The fraction of aptamers that are bound at equilibrium, defined as θ , is then:

$$\theta = \frac{[\text{AT}]_{\text{eq}}}{A_{\text{total}}},$$

where the dissociation constant K_d is given by:

$$K_d = \frac{k_{\text{off}}}{k_{\text{on}}}$$

Hence,

$$\theta = \frac{[\text{AT}]_{\text{eq}}}{A_{\text{total}}} = \frac{[\text{T}]}{K_d + [\text{T}]}$$

This expression is recognised as the classical Hill–Langmuir isotherm, which is a special case of the more general Langmuir equation. In scenarios where the binding is non-cooperative (i.e. the binding of one molecule does not influence the binding of another), the Hill coefficient n is equal to 1, and the binding curve is hyperbolic. However, if cooperative binding is present, the Hill–Langmuir isotherm takes the form:

$$\theta = \frac{[\text{AT}]_{\text{eq}}}{A_{\text{total}}} = \frac{[\text{T}]^n}{K_d^n + [\text{T}]^n}.$$

The introduction of the Hill coefficient n allows for the modelling of sigmoidal binding curves, which are often observed when multiple binding sites or cooperative interactions are involved. This sigmoidal behaviour is a direct manifestation of the underlying cooperative mechanisms that govern the sensor's response to varying target concentrations.

In simulating the operation of electrochemical aptamer-based sensors, the dynamic evolution of the aptamer–target complex is typically modelled by solving the differential equation derived earlier whilst the electrochemical current response associated with the concentration of the target can be modelled as a function of the fraction of bound aptamers. A linear relationship is often assumed:

$$I = I_{\min} + (I_{\max} - I_{\min}) \cdot \theta$$

Where considering the cooperative/non-cooperative factor and Hill coefficient the equation will be:

$$I = I_{\min} + (I_{\max} - I_{\min}) \cdot \frac{[T]^n}{K_d^n + [T]^n}$$

In the equation above with $\theta \rightarrow 1$ the current (I) reaches its maximum I_{\max} whereas, with $\theta \rightarrow 0$ the equation becomes $I = I_{\min}$ while the shape of the I vs. $[T]$ might retain its sigmoidal formation.

It worths to be noted that even in the absence of cooperative interactions (i.e. $n = 1$), plotting the binding response against the logarithm of the target concentration can produce a sigmoidal appearance. This effect arises from the compression of low-concentration data and the expansion of mid-range values, thereby accentuating the transition between the unbound and bound states. Both these factors must be taken into account when interpreting the results of sensor simulations and fitting experimental data to the Hill–Langmuir model.

While our initial approach offers a charmingly straightforward view—linking the sensor current directly to the fraction of bound aptamers—this simplicity glosses over the intricate details of electron transfer. Think of it as using a single snapshot to describe a dance that's actually a full-blown performance. In our basic model, we assume that the sensor's current changes linearly as more aptamers bind their target. which works well as a first approximation. However, the real world of electron transfer isn't always so cooperative—it can be as temperamental as a diva on stage. There are events that may contribute to the current signal which might need to be included to the simulation model for more accurate estimation of the parameters involved in the overall kinetics mechanism ruling the system. the key events that can influence the electrochemical kinetics in an aptamer-based, “signal-on” sensor, where the aptamer bends toward the electrode upon target binding, bringing the redox label (e.g. methylene blue) closer to the electrode:

1. Aptamer Conformational change: When the target binds, the aptamer folds or “bends” in such a way that redox label is brought closer to the electrode surface. This change can drastically alter the electron-transfer rate given the fact that the closer redox label is to the electrode, the faster electron transfer can occur and vice versa.
2. Electron-Transfer Kinetics (Redox Reaction at the Electrode): The redox label must undergo electron transfer with the electrode (e. g. gold electrode). The electrode in the E-AB sensors also plays a role of substrate that the tagged-aptamer is bound to via a thiolated terminal to the electrode surface. In a classical electrochemical sense, the

electron-transfer and the measured current can be formulated by Butler–Volmer or Marcus theory which will be discussed later, however, If the redox label is distant from the electrode (unbound state), the electron transfer consequently becomes sluggish and in the bound state a more facile electron-transfer is expected. This electron-transfer step is often quite fast (microseconds to milliseconds), but it's modulated by the effective distance/orientation of redox label relative to the electrode.

3. Double-Layer Charging or Interfacial Capacitance: Any electrode–solution interface forms a double layer upon applying potential to the electrode (namely the working electrode) which is essentially due to [a brief discussion is required here]. Upon applying the potential, the charge partially goes into charging or discharging the interfacial capacitance. Given the SWV as the sensor interrogating technique, at higher frequencies, significant current can be “lost” to charging the double layer rather than contributing to the faradaic (redox) reaction. This is often captured in the “decay” factor of frequency-dependent models. The double-layer charge/discharge typically occurs in the microseconds to milliseconds range, depending on electrode area, ionic strength, and surface coverage of aptamers.
4. Mass Transport (Diffusion, Convection): If the target diffusion to/from the electrode and mass transport can limit the overall kinetic rate. In many aptamer sensors, the aptamer is pre-immobilised, and the redox label is covalently attached, so the main mass transport might be for the target binding event or background redox mediators. Repeatedly scanning at high frequency could potentially lead to local depletion or in some case accumulation altering the measured signal. Diffusion-limited processes are typically slower than pure electron-transfer steps, however, for a surface-bound aptamer, mass transport is often less critical once the aptamer is loaded.
5. Non-Specific Adsorption or Partial Blocking: non-relevant species in the solution might adsorb to the gold surface or even partially block the aptamer. The aptamer itself can also pack more densely over time, or the target might cause a secondary blocking effect. Changes in effective surface area, local environment, or orientation of the aptamer can introduce additional “penalties” to electron transfer or alter the double-layer capacitance. This passivation event can be relatively slow (seconds to minutes), but it can manifest as a systematic drift in the data if you measure for extended periods.

While the abovementioned events might contribute to the overall measured current, however, the contribution and significant of each to the current experimentally measured might be disputable and perhaps the less significant event might be omitted in the simulation model. On the other hand, some aptamer might be getting involved in a multi-step conformational Pathways where the aptamer might not simply flip from “unbound” to “bound” and might adopt to intermediate conformations or partial folds. This might be represented as multiple distinct time constants in the collected data—one for the initial partial fold, another for the final docking onto the electrode. In a frequency-sweep experiment, these separate events can appear as multiple exponential decays. While such scenarios might in reality be involved in the aptamer capturing mechanisms, however, this might be a subject of another discussion and for now will be skipped out from the simulation algorithm.

In the well-established approach for E-AB sensors presumably at a single operating frequency or at equilibrium as mentioned above is: $I = I_{\min} + (I_{\max} - I_{\min}) \theta$,
 $\theta = \frac{[T]}{K_D + [T]}$

This equation captures how the sensor's measured current (I) transitions from I_{\min} (fully unbound) to I_{\max} (fully bound) as more aptamers bind. However, that form does not by

itself describe how the amplitude changes when the sensor is driven **at various frequencies in SWV**. In practice, one might measure the unbound condition (negligible target) and a saturating bound condition (high target concentration) at a series of frequencies. Each condition then yields a distinct frequency-dependent curve. To capture these frequency effects, we introduce models in which the measured amplitude (peak current or integrated charge) is modified by the limited time per half-cycle of SWV and by electron-transfer kinetics. A simple phenomenological version uses multiple exponential “penalties” in series:

$$I_{\text{net}}(f) = I_0 \exp\left(-\frac{k_{\text{et}}}{2f}\right) \exp\left(-\frac{f}{f_{\text{conf}}}\right) \exp\left(-\frac{f}{f_{\text{DL}}}\right) \exp\left(-\frac{f}{f_{\text{mass}}}\right) \exp\left(-\frac{f}{f_{\text{ads}}}\right)$$

Where:

- I_0 is an overall scaling factor (possibly also fitted).
- $\exp(-k_{\text{et}}/(2f))$ captures the electron-transfer kinetics that often appear in SWV modelling (the $1/(2f)$ factor is a heuristic).
- $\exp(-f/f_{\text{conf}})$ could be a rough proxy for how aptamer conformational gating becomes less effective at higher frequencies (there’s less time for the aptamer to fold “signal-on”).
- $\exp(-f/f_{\text{DL}})$ the effect of double-layer charging at high frequencies.
- $\exp(-f/f_{\text{mass}})$ might account for mass-transport or diffusion limitations.
- $\exp(-f/f_{\text{ads}})$ could represent partial blocking or slow fouling processes that reduce the current with increasing frequency.

For the sake of simplicity in the simulation model, considering the fact that f_{conf} plays a major role while f_{DL} , f_{mass} and f_{ads} relatively a minor role, the equation can be re-written as:

$$I_{\text{net}}(f) = I_0 \exp\left(-\frac{k_{\text{et}}}{2f}\right) \exp\left(-\frac{f}{f_{\text{conf}}}\right) \exp\left(-\frac{f}{f_{\text{others}}}\right),$$

where I_0 sets a baseline amplitude, $\exp(-k_{\text{et}}/(2f))$ accounts for an electron-transfer gating that is suppressed at higher frequencies, and $\exp(-f/f_{\text{conf}})\exp(-f/f_{\text{others}})$ lumps together phenomena such as conformational gating, double-layer charging, mass transport, and adsorption/passivation effects. For each state (unbound vs. bound), a separate set of parameters $\{I_0, k_{\text{et}}, f_{\text{conf}}, f_{\text{others}}\}$ hence can be fitted. In the low-frequency, the exponentials all tend to 1, so the amplitude approaches a constant—analogueous to I_{min} or I_{max} from the fraction-bound viewpoint.

Because a purely mathematical multi-exponential may lack direct physical interpretation of electron-transfer kinetics, we then adopt more electrochemically grounded expressions. The Butler–Volmer equation, a macroscopic workhorse in electrochemistry, relates the current density j to the overpotential η by considering both the forward and reverse electron transfer reactions. In a Butler–Volmer framework, the redox current density $j_{\text{BV}}(\eta)$ is:

$$j_{\text{BV}}(\eta) = j_0 \left[\exp\left(\frac{(1-\alpha)F\eta}{RT}\right) - \exp\left(-\frac{\alpha F\eta}{RT}\right) \right],$$

where j_0 is the exchange current density, α the charge-transfer coefficient, and η the overpotential. To replicate the “rise-then-fall” shape seen in experimental SWV amplitude vs.

frequency, one introduces a frequency-dependent effective overpotential, $\eta_{\text{eff}}(f)$ which is near 0 at low frequency and saturates to some η_0 at mid/high frequency. A common choice is then:

$$\eta_{\text{eff}}(f) = \eta_0 (1 - \exp(-\frac{k_{\text{freq}}}{f})),$$

so that the Butler–Volmer term starts small and rises before additional exponential decay factors eventually drive the amplitude back down at higher frequencies. The overall current then becomes:

$$I_{\text{net}}(f) = I_0 j_{\text{BV}}(\eta_{\text{eff}}(f)) \exp(-\frac{f}{f_{\text{conf}}}) \exp(-\frac{f}{f_{\text{others}}}).$$

On a more microscopic level, Marcus theory dives into the quantum mechanics of electron transfer. It tells us that the rate of electron transfer, k_{et} depends crucially on the reorganisation energy λ (the energy needed to rearrange the surrounding molecular environment) and the free energy change ΔG° .

$$k_{\text{et,base}} = A_{\text{Marcus}} \exp[-\frac{(\lambda + \Delta G^\circ)^2}{4\lambda k_B T}],$$

where A is a pre-exponential factor and K_B is Boltzmann's constant. Marcus theory introduces the fascinating concept of an "inverted region"—a regime where increasing the driving force (making ΔG° more negative) can actually slow down the electron transfer rate. This counterintuitive insight is something our simplified model would never hint at. To allow a frequency-dependent rise, a multiplicative factor such as $[1 - \exp(-f/k_{\text{freq}})]$ is introduced, ensuring that $k_{\text{et}}(f) \approx 0$ at very low frequency and saturates at $k_{\text{et,base}}$ for mid/high frequency. The final amplitude is

$$I_{\text{net}}(f) = I_0 k_{\text{et}}(f) \exp(-\frac{f}{f_{\text{conf}}}) \exp(-\frac{f}{f_{\text{others}}}).$$

As with Butler–Volmer, each state (unbound vs. bound) can differ in ΔG_0 or other parameters, giving two distinct frequency-response curves that cross over in the experimental data.

In all these approaches, one obtains a frequency-domain expression that gracefully covers the low-frequency limit (where the sensor current saturates near a constant) and high-frequency regime (where exponential penalties suppress the amplitude). This aligns with the fraction-bound concept in the sense that aptamer in a signal-on mechanism and at very low frequencies, the sensor has enough time to adopt its “fully bound” or “fully unbound” conformation, giving an amplitude close to I_{max} or I_{min} . At intermediate frequencies, faster electron-transfer routes (the bound state) can maintain higher currents, whereas slower ones (the unbound state) begin to lose amplitude. Eventually, at high frequencies, additional processes such as incomplete conformational gating, double-layer charging, mass transport, or adsorption/passivation effects drive both states down.

Hence, the fraction-bound model denoted as $I = I_{\text{min}} + (I_{\text{max}} - I_{\text{min}}) \theta$ describes how aptamer binding controls the equilibrium amplitude, while the frequency-dependent BV or Marcus models elaborate on how that amplitude is further modulated by limited electron-transfer time per cycle. Furthermore, if partial target concentrations were measured, one could combine the fraction-bound logic with frequency dependence by mixing the two states proportionally, but often just measuring the two extremes (unbound vs. bound) suffices to highlight how kinetics differ.

Finally, whether the experimental observable is **peak current** or **integrated charge** under the SWV peak does not alter the fundamental approach. Both metrics reflect the net electron-transfer event each cycle. The user can normalise and fit these data points against frequency with the same equations, so long as a single amplitude value is extracted per frequency. In practice, integrated charge can sometimes better capture sluggish kinetics, whereas peak current may be more directly read from the SWV curve. The essential requirement is that each frequency yields one amplitude for the unbound state and one for the bound state, and these are fitted to physically motivated models that incorporate electron-transfer constraints plus other frequency penalties.